Inherently Electroactive Graphene Oxide Nanoplatelets As Labels for Single Nucleotide Polymorphism Detection

Alessandra Bonanni,[†] Chun Kiang Chua,[†] Guanjia Zhao,[†] Zdeněk Sofer,[‡] and Martin Pumera[†,*]

[†]Division of Chemistry & Biological Chemistry, School of Physical and Mathematical Sciences, Nanyang Technological University, Singapore 637371 and [‡]Department of Inorganic Chemistry, Institute of Chemical Technology, 166 28 Prague 6, Czech Republic

ABSTRACT Graphene materials are being widely used in electrochemistry due to their versatility and excellent properties as platforms for biosensing. However, no records show the use of inherent redox properties of graphene oxide as a label for detection. Here for the first time we used graphene oxide nanoplatelets (GONPs) as electroactive labels for DNA analysis. The working signal comes from the reduction of the oxygen-containing groups present on the surface of GONPs. The different ability of the graphene oxide nanoplatelets to conjugate to DNA hybrids obtained with complementary, noncomplementary, and one-mismatch sequences allows the discrimination of single-nucleotide polymorphism correlated with Alzheimer's disease. We believe that our findings are very important to open a new route in the use of graphene oxide in electrochemistry.

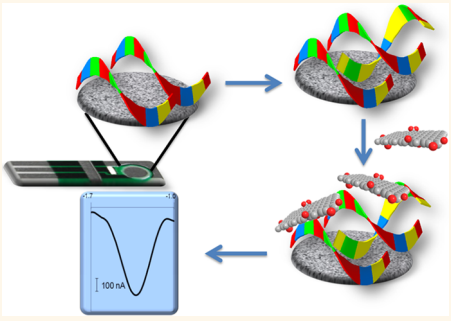

KEYWORDS: electroactive graphene oxide · genosensor · single-nucleotide polymorphism · graphene label

Graphene and graphene-related materials, such as graphene oxides, have been attracting great interest from the scientific community due to their interesting electronic, mechanical, thermal, optical, and electrochemical properties. Graphene is an excellent surface for electrochemistry,[1−3] and it is often used as an electrode material in sensing[4−6] and energy storage[7−9] applications. Graphene is inherently redox inactive at typically used potentials, which means that graphene does not show any electrochemically driven redox (oxidation/reduction) behaviors. On the contrary, graphene oxide (GO) materials display an inherent redox activity that allows for their electrochemical reduction toward reduced graphenes.[10] Note that the term "graphene oxide" refers to graphene sheets that were oxidized with various oxygen-containing groups, such as hydroxyl, aldehyde, epoxy, carboxyl, carbonyl, and peroxy.[11] The electrochemical reduction method of graphene oxide is used for preparation of electrode surfaces[12,13] or for quantification of reducible oxygen-containing groups.[14,15] However, there have not been any attempts shown that utilize the inherent electrochemical redox activity of graphene oxide as a label for DNA detection.

Here we exploit the unique inherent electroactivity of graphene oxide nanoplatelets (GONPs) for DNA and single-base polymorphism detection. The use of graphene oxide nanoplatelets with a high density of oxygen functionalities is beneficial over standard probes, as the signal amplification is very large, whereby a 50 × 50 nm sized graphene oxide platelet corresponds to almost 22 000 withdrawn electrons (given the density of reducible groups of 4.3 nm^{-1} and two-electron reduction per functional group).[14] We also explore the unique interaction between graphene oxide nanoplatelets and single-stranded DNA nitrogenous bases, which differs significantly from its interaction with double-stranded DNA due to the shielding of the bases inside the double helix.[16] To the best of our knowledge, this is the first time the reduction peak of GO is used as the analytical signal in general.

In particular, in this work complementary (wild-type), noncomplementary (nc), and one-mismatch (mutant) DNA sequences were employed for the hybridization of the electrode surface modified with DNA probes. After the hybridization steps, the electrode surfaces were incubated with a solution

* Address correspondence to pumera@ntu.edu.sg.

Received for review March 28, 2012 and accepted September 19, 2012.

Published online September 19, 2012
10.1021/nn301359y

© 2012 American Chemical Society

containing a certain amount of GONPs. The different conjugation ability of graphene with single- and double-stranded DNA (dsDNA) sequences was exploited here. It is well known that single-stranded DNA (ssDNA) sequences lie on the surfaces of graphene sheets *via* $\pi-\pi$ stacking interactions.[17,18] It was also shown that ssDNA and dsDNA possessed different binding affinities for graphene, with the former being more suitable to this aim.[19,20] In fact, while the nitrogenous bases in ssDNA are free to form $\pi-\pi$ stacking with graphene aromatic rings, the dsDNA nitrogenous bases are less accessible for interactions since they are shielded inside the double-helix structure. The different binding ability of GONPs to DNA hybrids formed with complementary, noncomplementary, and mismatch-containing sequences would result in a different amount of GONPs conjugated to the electrode surface upon incubation. As such, this could provide different electrochemical signals to discriminate among wild-type, mutant, and noncomplementary DNA in a simple and fast protocol.

RESULTS AND DISCUSSION

We explore here the unique interactions between graphene oxide nanoplatelets and DNA strands for single-nucleotide polymorphism detection. We demonstrate that single-stranded and double-stranded DNA interact in different fashions with graphene oxide nanoplatelets. Consequently, we exploit the unique properties of graphene oxide as inherently electroactive labels.

GONPs were obtained by ultrasonication[21] of an aqueous solution of graphite oxide nanoplatelets obtained from the oxidation of commercial graphite nanofibers by the modified Hummers' method.[22] In order to gain more insights into the material used for DNA labeling, the GONPs used in these experiments were characterized by scanning electron microscopy (SEM), high-resolution transmission electron microscopy (HR-TEM), atomic force microscopy (AFM), and electrochemistry.

The SEM image shows the filamentous structure of the fiber with uniform size distribution (Figure 1a). The HR-TEM image showed that the graphene sheets were perpendicularly aligned along the fiber axis (Figure 1b). The average observed diameter was around 35 nm. After the exfoliation by ultrasonication, the fibrous structure disappeared and gave separate individual graphene oxide nanoplatelets instead. The AFM image and height profile confirmed the presence of individual nanoplatelets with an average thickness around 1.2 nm (Figure 1c). Figure 1d shows the colloidal suspension of graphite nanofibers (GNFs) and GONPs after being sonicated for 30 min. As seen in the picture, GNFs were deposited on the bottom of the bottle, while GONPs form a very stable suspension[23] (picture taken on the third day after preparation). The good stability of the

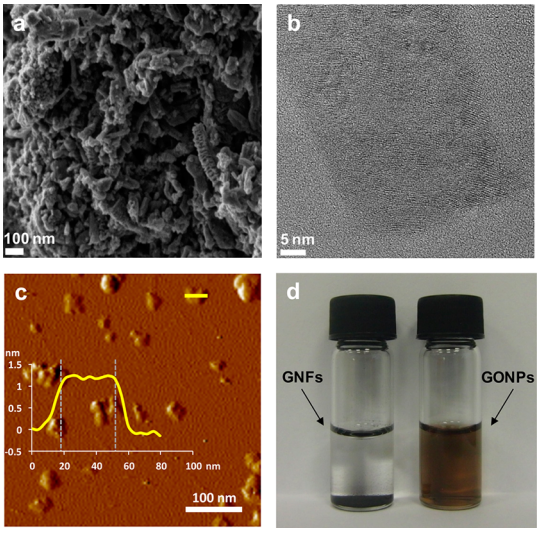

Figure 1. Microscopy characterizations of GNFs and GONPs. (a and b) SEM and HR-TEM images of the graphite nanofibers as received. (c) AFM image and height profile of exfoliated GONPs. (d) Colloidal suspension of graphite nanofibers (GNFs) as received and GONPs after oxidation/exfoliation.

GONPs was due to their zeta potential of −41.5 mV ($n = 3$). ASTM defines colloids with a zeta potential higher than 40 mV (in absolute value) as having good stability.[24] GNFs showed a ζ potential of +30.9 mV ($n = 3$), indicating that the low ζ potential is the reason for poor stability of its colloids. SEM and TEM images of the material before and after oxidation/exfoliation and a more detailed AFM characterization are shown in the Supporting Information (see Figures S1, S2, S3). The size distribution of GONPs was measured by dynamic light scattering (see Figure S4) and gives an average size value of 37 nm, which closely corresponds to the average diameter of starting carbon fibers as well as to the diameter of GONPs measured by AFM. The whole characterization of GNFs as received and GONPs confirmed that the fibers were digested, and no nanofiber structure is shown after the oxidation/exfoliation treatment.

We then investigated the electrochemical behavior of GONPs by performing cyclic voltammetry between −0.2 and −2.0 V. As illustrated in Figure 2, two cyclic voltammetric waves between −1 and −1.5 V appeared in the first scan, corresponding to the reduction of the different oxygen-containing groups on the GONP surface, such as epoxy, aldehyde, and peroxy.[14] This reduction signal was used as the working signal for biosensing purposes. The differential pulse voltammetry (DPV) technique was then employed, as it shows better sensitivity when compared to cyclic voltammetry.[25] A calibration curve for different GONP concentrations was obtained by DPV. The obtained signal increased linearly with increasing concentrations of GONPs (as shown in Figure S5, Supporting Information).

Following the electrochemical characterizations, GONPs were used as an electrochemical-active label

for genosensing. Scheme 1 shows the detection procedure steps. First, DNA probes were immobilized on the electrode surface by physical adsorption.[26] Then, three different hybridization experiments were performed. The probe-modified electrode was incubated in three different solutions containing (A) complementary target (wild-type); (B) one-mismatch-containing sequence (mutant); and (C) noncomplementary target (nc). After hybridization was achieved, the three different electrode surfaces were incubated in a solution containing a specified amount of GONPs. As illustrated in Scheme 1, GONPs conjugate to the DNA-modified electrode surfaces to varying extents depending on the specific targets used in the hybridization step. For this reason, a different amount of GONPs was immobilized on the DNA-modified electrode surfaces, thus providing different voltammetric signals.

More specifically, when the hybridization step was performed with the complementary target, a low amount of GONPs was conjugated to the DNA-modified electrode surface and gave rise to a small reduction signal, as shown by the voltammetric peak (wild-type, red line). For hybridization with the one-mismatch sequence, the amount of GONPs bound to the DNA-modified electrode surface increased, and this resulted in a higher voltammetric peak (mutant, blue line). Finally, the highest electrochemical signal was given by the electrode surface that was incubated in the noncomplementary target solution (nc, black line).

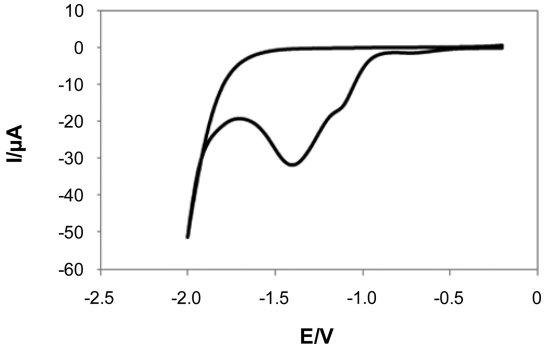

Figure 2. Graphene oxide nanoplatelets show an inherent electrochemical reduction signal. Cyclic voltammogram for the electrochemical reduction of GONPs in 10 mM phosphate buffer solution, pH 7.0. Scan rate: 20 mV s^{-1}. Reference electrode: Ag/AgCl.

These different behaviors could be attributed to the different binding affinity of graphene nanoplatelets toward single- and double-stranded DNA. Upon hybridization with the complementary target, the electrode surface was modified with a significant amount of dsDNA sequences, while in the case of the noncomplementary target the electrode surface consisted mainly of nonhybridized ssDNA probes. Since as already explained, graphene possesses a stronger ability to conjugate to ssDNA, a higher amount of GONPs will be detected on the electrode surface that was incubated with the noncomplementary target. In the case of the one-mismatch sequence the voltammetric signal was higher than the complementary target one, due to the partial hybridization occurring on the electrode surface.

Chronocoulometry experiments were performed to establish the DNA density on the electrode surface after the hybridization step. The results confirmed our hypothesis (see Figure S6, Supporting Information), the DNA density on the electrode modified with the DNA complementary target being 2.53×10^{13} molecules/cm^2, much higher than on the mutant (2.40×10^{13} molecules/cm^2) and on the noncomplementary target (2.28×10^{13} molecules/cm^2).

In order to optimize the amount of DNA to be used in the hybridization steps and to evaluate the limit of

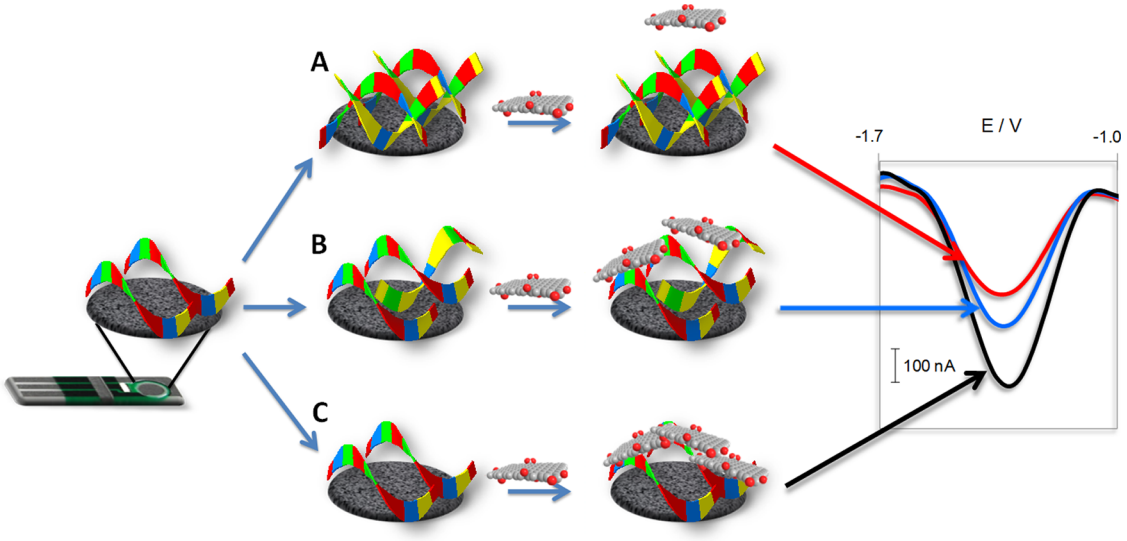

Scheme 1. Schematic of the experimental protocol. The hybridization step was performed with complementary target (A); one-mismatch target (B); and noncomplementary target (C).

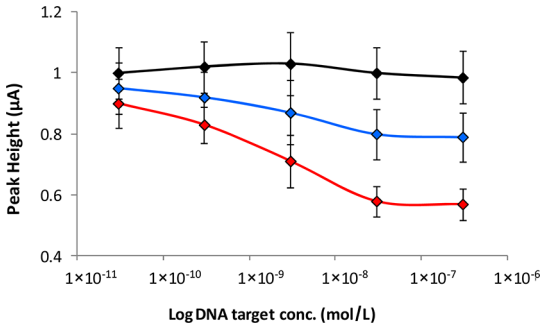

Figure 3. Voltammetric response toward the DNA target concentration in the case of hybridization with wild-type (red diamonds), mutant (blue diamonds), and noncomplementary (black diamonds) targets. Error bars represent triplicate experiments. Individual values are shown in Table S1 (Supporting Information).

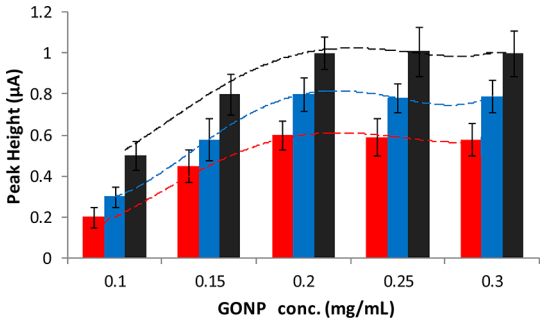

Figure 4. Voltammetric signal obtained after conjugation with different amounts of GONPs. Hybridization with wild-type (red histograms), mutant (blue histograms), and nc (black histograms) sequences. Error bars represent triplicate experiments. Individual values are shown in Table S2 (Supporting Information).

detection of the proposed biosensor, the variation of the GONP voltammetric signal *versus* DNA target concentration was studied. As illustrated in Figure 3, for the experiments with the complementary (red diamonds) and the mutant (blue diamonds) sequences, the voltammetric peak heights decreased with increasing concentration of DNA target until a plateau was reached at around 30 nM. At that point, further increment of DNA target concentration did not correspond to any signal decrement. The estimated limit of detection, calculated with consideration of the noise to be 3 times as high as the standard deviation of the value obtained in negative control experiments, was 500 pM. The differentiation between the wild-type and mutant was detectable to 10 nM. It is expected that with further development of this proof-of-concept principle the limit of detection could be significantly improved.

To establish the proper amount of GONPs for the labeling step, a calibration with different concentrations of GONPs was performed. The DNA target concentration was kept constant at a value of 30 nM. The histograms shown in Figure 4 represent the voltammetric peak height of GONP reduction *versus* the different GONP concentrations for hybridization with

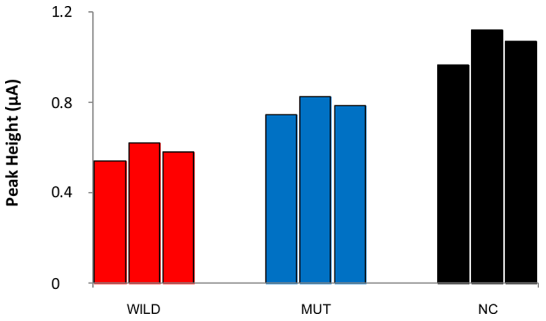

Figure 5. Histograms representing the peak height values obtained for the conjugation of GONPs with the different DNA target-modified electrode surfaces. Measurements were performed and are shown in triplicate. Concentration of DNA targets used in the experiments: 30 nM. Concentration of GONPs: 0.2 mg/mL.

the wild-type (red color), mutant (blue color), and nc (black color) sequences. As illustrated in Figure 4, the peak height increased when increasing the concentration of GONPs until a plateau was obtained at 0.2 mg/mL. This point corresponded to the maximum discrimination between the wild-type, mutant, and nc sequences. For higher concentrations of GONPs, there was no corresponding increase in the voltammetric peak. This indicated that the DNA-modified electrode surface was saturated with GONPs at a concentration of 0.2 mg/mL.

The optimized values of DNA target and GONPs were employed for the detection of DNA hybridization and polymorphism. In Figure 5, histograms representing the peak height of GONPs reduction *versus* the different hybridization experiments are shown. As seen in the figure, the discrimination between wild-type, mutant, and nc sequences was achieved with good reproducibility (RSD < 10%). Moreover, a 26% increase in the signal for mutant and 45% for noncomplementary sequence as compared to the complementary one was obtained. In addition, Student's *t* test was applied to compare the results obtained in the three hybridization experiments. The difference between the mean values was significant for all cases analyzed, being $t_{calc} > 6.41$ for all examined cases, larger than $t_{tab} = 2.13$, at the 95% confidence level, 4 degrees of freedom. This confirms that there is a very significant difference among the signals obtained for the three hybridization experiments.

The stability of the biosensor modified with the biorecognition element was studied for a time range of 4 weeks. On day 1 the electrode was modified with the optimized concentration of DNA probes. Hybridization experiments were realized on the same day (day no. 1) and after 2, 5, 7, 10, 14, 21, and 28 days. Results indicate a good stability of the electrode surface within two-weeks time (variation of the signal in the range of 10% standard deviation with respect to the first-day experiment). After 3 weeks a 10% decrease in the signal was observed. After 4 weeks the recorded signal decrease was 12% and also an increase in the

RSD% value was observed (see Supporting Information, Figure S7).

The response of GONPs as electroactive labels was also studied for different ultrasonication times employed during the preparation of the nanoplatelets. It is in fact well known that a prolonged ultrasonication can influence the resulting material shape and size.[27,28] For this reason GONPs obtained after 2, 8, 16, and 24 h ultrasonication were employed for the biosensing. The results, illustrated in Figure S8, show that when increasing the ultrasonication time from 2 h up to 24 h, both the electrochemical signal and the discrimination ability for complementary, noncomplementary, and mutant sequences worsen, with the 2 h ultrasonication time being the condition that provides the best results.

CONCLUSIONS

To conclude, we showed the proof of principle for the use of graphene nanoplatelets as electroactive labels for biosensors. We showed that ssDNA interacts with graphene oxide nanoplatelets in a different manner than dsDNA. This leads to the sensitive discrimination of the single-base mutation in the DNA sequence related to Alzheimer's disease. The reduction signal of graphene oxide nanoplatelets was exploited for the detection of DNA hybridization and polymorphism in a very simple and rapid protocol, by using disposable screen-printed electrodes.

The use of nanoplatelets, which are much smaller than regular size graphene sheets, allows for a better conjugation to DNA-modified electrode surfaces and improves the discrimination between single- and double-stranded DNA, which enables differentiation among complementary, noncomplementary, and one-mismatch DNA sequences correlated with Alzheimer's disease.

A completely new approach in the use of graphene was proposed in this work, showing that the material can be employed not only as a platform for biomolecule immobilization and analysis but also as a label either for its direct detection or for signal enhancement. Our findings are expected to have a profound impact on point-of-care personalized healthcare.

EXPERIMENTAL SECTION

Materials. Stacked graphite nanofibers were purchased from Strem Chemicals (Newburyport, MA, USA). Potassium ferricyanide ($K_3[Fe(CN)_6]$), potassium ferrocyanide ($K_4[Fe(CN)_6]$), tris-(hydroxymethyl)aminomethane (Tris), hexaammineruthenium(III) chloride, sulfuric acid (95−98%), potassium permanganate, sodium nitrate, hydrogen peroxide, and DNA sequences correlated with Alzheimer's disease were purchased from Sigma-Aldrich (Singapore). Buffer solutions used in the study are the following: 0.1 M PBS (0.1 M NaCl, 10 mM sodium phosphate buffer, pH 7.0), TSC1 (0.75 M NaCl, 75 mM trisodium citrate, pH 7.0), TSC2 (0.30 M NaCl, 30 mM trisodium citrate, pH 7.0), and Tris-HCl (10 mM Tris, pH 7.4). All solutions were made up using Milli-Q water (18.2 MΩ cm resistivity). The following oligonucleotide sequences were employed: DNA probe 5′-ACCAGGCGGCCGCACACGTCCTCCAT-3′; complementary target 5′-ATGGAGGACGTGTGCGGCCGCCTGGT-3′ (wild-type); 1-mismatch target 5′-ATGGAGGACGTG**C**GCGGCCGCCTGGT-3 (mutant); noncomplementary target 5′-AAAAAAAAAAAAAAAAAAAAAAAA-AA-3′ (nc). Oligonucleotides were diluted from stock solutions with sterilized Milli-Q water, separated into fractions, and stored at −20 °C. A single fraction was defrosted when required. Disposable electrical-printed carbon electrodes (DEP-chips, EE-PP model) were purchased from Biodevice Technology (Nomi, Japan). The three-electrode system included a carbon-based working electrode (2.64 mm^2 area), a Ag/AgCl reference electrode, and a carbon-based counter electrode.

Equipment. A JEOL-7600F semi-in-lens FE-SEM, operating in gentle-beam mode at 2 kV, was used to acquire the SEM images. AFM analysis was performed using a scanning probe microscope (model Multimode V by Veeco, Plainview, NY, USA). HR-TEM images were taken using a JEM 2100F field emission and Hitachi H-800 transmission electron microscope (JEOL, Japan). Size distribution and zeta potential were measured by a Zetasizer Nano ZS (Malvern) using dynamic light scattering and by laser Doppler microelectrophoresis, respectively. All electrochemical experiments were performed by using an Autolab PGSTAT302 potentiostat (Eco Chemie, Utrecht, The Netherlands) driven by GPES software, version 4.9. DPV measurements were performed in PBS buffer solution. Impedance measurements were recorded between 0.1 MHz and 0.1 Hz at a sinusoidal voltage perturbation of 10 mV amplitude. The experiments were carried out at an applied potential of 0.18 V (*vs* a Ag/AgCl reference electrode) in a 0.1 M PBS buffer solution containing 10 mM $K_3[Fe(CN)_6]$/$K_4[Fe(CN)_6]$ (1:1 molar ratio) as a redox probe.

Procedures. Graphene oxide nanoplatelets were produced in bulk quantities by following conventional protocols:[29] (a) a modified Hummers' method was employed to obtain graphite oxide nanoplatelets from graphite nanofibers.[22,30] A mixture of $NaNO_3$, H_2SO_4, and $KMnO_4$ was used for the oxidation of graphite nanofibers. (b) The obtained graphite oxide powder was dispersed in ultrapure water and then ultrasonicated for 3 h in order to obtain graphene oxide nanoplatelets.[21] More details on the procedures are available in the Supporting Information. For calibration curve purposes 3 μL of GONP suspension in milli-Q water at different concentrations was drop-casted onto each DEP-chip surface, and the solvent was allowed to dry at room temperature.

DNA probes were immobilized onto the electrode surface by dry physical adsorption. A 3 μL volume of DNA probe solution in PBS buffer solution at the optimized concentration of 10 μM (as resulted from impedance spectroscopy experiments,[31,32] see Figure S9 in the Supporting Information) was deposited onto the electrode surface for 10 min at 60 °C. The electrode was washed twice in PBS buffer with gentle stirring at room temperature to remove excess, nonadsorbed material. DEP-chips modified with DNA probes were incubated in an Eppendorf tube with the hybridization solution (TSC1 buffer) containing the desired concentration of DNA target (total volume 100 μL). The incubation was performed at 42 °C for 30 min, with gentle stirring. Two brief washing steps were then performed in TSC2 buffer at 42 °C. Incubation with GONPs was performed in an Eppendorf tube containing 100 μL of GONPs at the desired concentration in PBS solution. The incubation was performed at room temperature for 20 min, with gentle stirring. This was followed by two brief washing steps in PBS buffer.

DNA oligonucleotide surface density was determined by chronocoulometry according to the method reported by Steel *et al.*[33] The hexaammineruthenium(III) dilution in Tris-HCl buffer used in the experiments was optimized at 100 μM (as determined by measuring the binding isotherm of the DNA probe-modified platform). The DNA density on the electrode surface was calculated using the Cottrell equation and by considering the extrapolation of the intercept at time zero.

Conflict of Interest: The authors declare no competing financial interest.

Supporting Information Available: AFM, SEM, TEM, dynamic light scattering, chronocoulometry, and stability study. This material is available free of charge *via* the Internet at http://pubs.acs.org.

REFERENCES AND NOTES

1. Pumera, M. Graphene-Based Nanomaterials and Their Electrochemistry. *Chem. Soc. Rev.* **2010**, *39*, 4146–4157.
2. Chen, D.; Tang, L. H.; Li, J. H. Graphene-Based Materials in Electrochemistry. *Chem. Soc. Rev.* **2010**, *39*, 3157–3180.
3. Shao, Y. Y.; Wang, J.; Wu, H.; Liu, J.; Aksay, I. A.; Lin, Y. H. Graphene Based Electrochemical Sensors and Biosensors: A Review. *Electroanalysis* **2010**, *22*, 1027–1036.
4. Lu, C. H.; Yang, H. H.; Zhu, C. L.; Chen, X.; Chen, G. N. A Graphene Platform for Sensing Biomolecules. *Angew. Chem., Int. Ed.* **2009**, *48*, 4785–4787.
5. Pumera, M.; Ambrosi, A.; Bonanni, A.; Chng, E. L. K.; Poh, H. L. Graphene for Electrochemical Sensing and Biosensing. *Trends Anal. Chem.* **2010**, *29*, 954–965.
6. Chen, Q. W.; Zhang, L. Y.; Chen, G. Facile Preparation of Graphene-Copper Nanoparticle Composite by *in Situ* Chemical Reduction for Electrochemical Sensing of Carbohydrates. *Anal. Chem.* **2012**, *84*, 171–178.
7. Hoffert, M. I.; Caldeira, K.; Benford, G.; Criswell, D. R.; Green, C.; Herzog, H.; Jain, A. K.; Kheshgi, H. S.; Lackner, K. S.; Lewis, J. S.; *et al.* Advanced Technology Paths to Global Climate Stability: Energy for a Greenhouse Planet. *Science* **2002**, *298*, 981–987.
8. Brownson, D. A. C.; Kampouris, D. K.; Banks, C. E. An Overview of Graphene in Energy Production and Storage Applications. *J. Power Sources* **2011**, *196*, 4873–4885.
9. Pumera, M. Electrochemistry of Graphene: New Horizons for Sensing and Energy Storage. *Chem. Rec.* **2009**, *9*, 211–223.
10. Zhou, M.; Wang, Y. L.; Zhai, Y. M.; Zhai, J. F.; Ren, W.; Wang, F. A.; Dong, S. J. Controlled Synthesis of Large-Area and Patterned Electrochemically Reduced Graphene Oxide Films. *Chem.—Eur. J.* **2009**, *15*, 6116–6120.
11. Dreyer, D. R.; Park, S.; Bielawski, C. W.; Ruoff, R. S. The Chemistry of Graphene Oxide. *Chem. Soc. Rev.* **2010**, *39*, 228–240.
12. Guo, H. L.; Wang, X. F.; Qian, Q. Y.; Wang, F. B.; Xia, X. H. A Green Approach to the Synthesis of Graphene Nanosheets. *ACS Nano* **2009**, *3*, 2653–2659.
13. Bonanni, A.; Ambrosi, A.; Pumera, M. Nucleic Acid Functionalized Graphene for Biosensing. *Chem.—Eur. J.* **2012**, *18*, 1668–1673.
14. Chng, E. L. K.; Pumera, M. Solid-State Electrochemistry of Graphene Oxides: Absolute Quantification of Reducible Groups Using Voltammetry. *Chem. Asian J.* **2011**, *6*, 2899–2901.
15. Bonanni, A.; Ambrosi, A.; Pumera, M. On Oxygen-Containing Groups in Chemically Modified Graphenes. *Chem.—Eur. J.* **2012**, *18*, 4541–4548.
16. Li, F.; Huang, Y.; Yang, Q.; Zhong, Z. T.; Li, D.; Wang, L. H.; Song, S. P.; Fan, C. H. A Graphene-Enhanced Molecular Beacon for Homogeneous DNA Detection. *Nanoscale* **2010**, *2*, 1021–1026.
17. Patil, A. J.; Vickery, J. L.; Scott, T. B.; Mann, S. Aqueous Stabilization and Self-Assembly of Graphene Sheets into Layered Bio-Nanocomposites Using DNA. *Adv. Mater.* **2009**, *21*, 3159–3164.
18. Tang, Z. W.; Wu, H.; Cort, J. R.; Buchko, G. W.; Zhang, Y. Y.; Shao, Y. Y.; Aksay, I. A.; Liu, J.; Lin, Y. H. Constraint of DNA on Functionalized Graphene Improves Its Biostability and Specificity. *Small* **2010**, *6*, 1205–1209.
19. Xu, Y. X.; Wu, Q. O.; Sun, Y. Q.; Bai, H.; Shi, G. Q. Three-Dimensional Self-Assembly of Graphene Oxide and DNA into Multifunctional Hydrogels. *ACS Nano* **2010**, *4*, 7358–7362.
20. Bonanni, A.; Pumera, M. Graphene Platform for Hairpin-DNA-Based Impedimetric Genosensing. *ACS Nano* **2011**, *5*, 2356–2361.
21. Paredes, J. I.; Villar-Rodil, S.; Martinez-Alonso, A.; Tascon, J. M. D. Graphene Oxide Dispersions in Organic Solvents. *Langmuir* **2008**, *24*, 10560–10564.
22. Hummers, W. S.; Offeman, R. E. Preparation of Graphitic Oxide. *J. Am. Chem. Soc.* **1958**, *80*, 1339–1339.
23. Park, S.; An, J. H.; Jung, I. W.; Piner, R. D.; An, S. J.; Li, X. S.; Velamakanni, A.; Ruoff, R. S. Colloidal Suspensions of Highly Reduced Graphene Oxide in a Wide Variety of Organic Solvents. *Nano Lett.* **2009**, *9*, 1593–1597.
24. Si, Y.; Samulski, E. T. Synthesis of Water Soluble Graphene. *Nano Lett.* **2008**, *8*, 1679–1682.
25. Compton, R. G.; Banks, C. E. *Understanding Voltammetry*, 2nd ed.; Imperial College Press: London, 2011; pp 348−350.
26. Bonanni, A.; Esplandiu, M. J.; Pividori, M. I.; Alegret, S.; del Valle, M. Impedimetric Genosensors for the Detection of DNA Hybridization. *Anal. Bioanal. Chem.* **2006**, *385*, 1195–1201.
27. Stankovich, S.; Piner, R. D.; Chen, X. Q.; Wu, N. Q.; Nguyen, S. T.; Ruoff, R. S. Stable Aqueous Dispersions of Graphitic Nanoplatelets *via* the Reduction of Exfoliated Graphite Oxide in the Presence of Poly(sodium 4-styrenesulfonate). *J. Mater. Chem.* **2006**, *16*, 155–158.
28. Park, S.; Ruoff, R. S. Chemical Methods for the Production of Graphenes. *Nat. Nanotechnol.* **2009**, *4*, 217–224.
29. Luo, J. Y.; Cote, L. J.; Tung, V. C.; Tan, A. T. L.; Goins, P. E.; Wu, J. S.; Huang, J. X. Graphene Oxide Nanocolloids. *J. Am. Chem. Soc.* **2010**, *132*, 17667–17669.
30. Cote, L. J.; Kim, F.; Huang, J. X. Langmuir-Blodgett Assembly of Graphite Oxide Single Layers. *J. Am. Chem. Soc.* **2009**, *131*, 1043–1049.
31. Bonanni, A.; Esplandiu, M. J.; del Valle, M. Signal Amplification for Impedimetric Genosensing Using Gold-Streptavidin Nanoparticles. *Electrochim. Acta* **2008**, *53*, 4022–4029.
32. Bonanni, A.; del Valle, M. Use of Nanomaterials for Impedimetric DNA Sensors: A Review. *Anal. Chim. Acta* **2010**, *678*, 7–17.
33. Steel, A. B.; Herne, T. M.; Tarlov, M. J. Electrochemical Quantitation of DNA Immobilized on Gold. *Anal. Chem.* **1998**, *70*, 4670–4677.